DOI: 10.13009/EUCASS2019-434

The High Level of Maturity of the elsA CFD Software for Aerodynamics Applications

Sylvie Plot
ONERA, University Paris Saclay
7-92322 Châtillon – France
Sylvie.plot@onera.fr

Abstract

The elsA CFD software developed at ONERA is both a software package capitalizing the innovative results of research over time and a multi-purpose tool for applied CFD and for multi-physics. elsA is used intensively by the Safran and Airbus groups and ONERA, as well as other industrial groups and research partners. This paper presents the main capabilities of elsA and recent numerical simulations using elsA for a wide range of challenging aeronautic applications. The simulations address aerodynamics computations as well as aero-structure and aeroacoustics ones. Each simulation enables to underline differentiating modelling and numerical methods implemented within elsA and shows that this software has reached a very high level of maturity and reliability.

Nomenclature

CFD	Computational Fluid Dynamics
elsA	ensemble Logiciel de Simulation en Aérodynamique
UHB/UHBR	Ultra-High Bypass/Ultra-High Bypass Ratio
CROR	contra rotating open rotor
(U)RANS	(unsteady) Reynolds Averaged Navier-Stokes
EARSM/DRSM	Explicit Algebraic/Differential Reynolds Stress Model
(Z)DES/LES	(Zonal) Detached/Large Eddy Simulation
DNS	Direct Numerical Simulation
OO	Object-Oriented
MFA	Multiple Frequency phase-lagged Approach

1. Introduction

Advanced CFD is one key differentiating factor for designing efficient transportation systems. Accuracy and efficiency are crucial for aeronautical manufacturers to optimize the design of their products so that the limit of the aircraft flight envelopes is extended. Accurate and robust numerical simulation capabilities are essential to take into account complex phenomena involved in flow physics and to simulate real complex geometries encountered in aeronautics. Numerical methods have to meet the constantly rising requirements in terms of efficiency in order to reduce the response time for complex simulations.

To this end, the Airbus and Safran groups use the elsA [1] software (ONERA-Airbus-Safran property), a multi-purpose tool for applied CFD and multi-physics. Indeed, while it is rather unusual for a CFD software package to deal both with external flows around aircrafts or helicopters and with internal flows in turbomachinery, elsA is today used as a reliable tool by Airbus for transport aircraft configurations [2][3] and helicopter applications [4][5], by Safran for turbomachinery flow simulations [6][7]. Among other industrial users, let us mention MBDA for missile configurations and Électricité de France for steam turbine applications [8][9].

The high levels of accuracy and reliability required today in aeronautic design are obtained through long term expertise and innovative research present at ONERA in various areas: physical modelling, algorithms, numerical methods, software efficiency on rapidly evolving hardware and validation and verification of aerodynamics results by comparison with detailed experimental data. The elsA software benefits directly from the above, as well as from multiple skills of many of its research partners. Among them the followings establishments have participated or participate to its development and validation mainly in the following indicated areas: Cerfacs for studies dealing in particular with numerical methods [10][11][12][13] and CPU efficiency [14] LMFA and LTDS labs of École Centrale de Lyon [15][16][17] for turbomachinery applications and special interests in acoustics and vibrations, Cenaero (Belgium) [18][19], the Von Karman Institute [20] and ISAE institute [21] for turbomachinery flow

DOI: 10.13009/EUCASS2019-434

simulation, the Dynfluid lab (Arts et Métiers ParisTech) for high accuracy numerical schemes [22], the Institute of Technology Antoine de Saint-Exupéry [23] and the Delft University of Technology [24] for design optimizations.

Among topics of prime importance when using CFD as a tool in aircraft, helicopter and turbomachine design one can mention the ability to handle the complexity of the geometries and the unsteadiness of the flows, the need to properly model the turbulence and accurately compute the onset of laminar-turbulent transition, the requirement of high fidelity simulations for instance to master acoustic issues, as well as the capability to compute the high-fidelity aeroelastic behaviour of aircraft and turbomachines, and the deformations occurring under loads. Hereafter an illustration of these different themes and their associated context is provided.

As for complex configurations, let us cite four examples. The assessment of the aerodynamics performance of a complete cruise aircraft configuration and specially the prediction of the drag is very challenging. One needs to be able to compute with high accuracy the flow around geometries containing wings, body, nacelles and pylons, and horizontal and vertical tails. This requires accurate numerical methods and the ability to deal with sophisticated meshes. In turbomachinery experimental and numerical studies have shown that taking into account geometrical components such as casing treatments, grooves, blade slots, cooling holes or gaps separating fixed and rotating walls can have a crucial impact on the performance of gas turbines. Therefore it is important for aeroengine designers to simulate more and more accurately the very complex geometries encountered on industrial turbomachines by integrating in the design process these geometrical components, at a reasonable cost. In today's context of an increased focus on fuel efficiency and environmental impact, UHBR engines become an interesting option but the resulting size of the nacelles pose challenges in terms of installation on the airframe and impact on overall performance. Aircraft manufacturers have to properly and efficiently compute engine integrated wing configurations. Rotorcraft are by nature complex machines, and the RACER, the Airbus Helicopters high-speed demonstrator with its lateral rotors also defined as propellers, providing anti-torque in hover and thrust in cruise flight is no exception to the rule. Several strategies and levels of numerical fidelity can be used to model the RACER propeller installation effects.

Besides, the turbulence modelling influences strongly the prediction of the secondary and leakage flows in turbomachinery. Yet the search of the highest efficiency and largest stable operating range of a turbomachinery for a given stagnation pressure ratio are design objectives for high pressure compressors and those quantities are directly and strongly impacted by the secondary and leakage flows occurring in the blade passage such as corner separation or stall and tip leakage flows. The laminar-turbulent transition modelling is also of prime importance. For instance, accurate computation of transport aircraft drag strongly relies on natural laminar-turbulent transition prediction capabilities. So it is necessary to exploit accurate transition prediction techniques compatible with CFD. Of course unsteadiness must also be addressed in the design process. The relative motion between adjacent rotor and stator blade rows present in turbomachinery configurations gives rise to a wide range of unsteady flow mechanisms such as wake interactions, potential effects, hot streak migrations, shock wave propagations, or unsteady transitional flows. All these phenomena can have a crucial impact on the performance of gas turbines and cannot be captured accurately with a steady mixing-plane approach since the averaging treatment at the rotor/stator interface filters all unsteady effects. Specific unsteady techniques exist for turbomachinery computations. Unsteadiness is not only due to motion between bodies or variable boundary conditions but is intrinsic to the turbulent nature of compressible flows. So depending on the problem one has to solve, the unsteadiness of turbulence must be taken into account. It is the case for instance for a jet noise study. One needs to rely on robust and accurate unsteady approaches to simulate the turbulent mechanisms which generate noise. In the loads and aeroelastic fields, specific gust response is considered as one of the most important loads encountered by an aircraft so that it is crucial to compute the high-fidelity aeroelastic gust response for a large range of flight points and mass configurations and for different critical gust shapes than an aircraft must withstand. Taking into account of the real manufactured blade shape in the investigation of the blade deformations due to centrifugal forces and aerodynamic loads during the flight is key for an accurate prediction of CROR performances for instance. In high-lift and especially landing conditions, massive flow separation might occur on aircraft wings and be responsible for dramatic wing stall and associated lift loss. It is thus important to be able to predict this phenomenon as well as to compute the resulting flows when using active flow control systems for determining relevant locations and settings of these devices. In the helicopter field, dynamic stall is a highly complex phenomenon characterized by unsteady massive separated flow. It limits the flight envelope of helicopters by generating vibrations and large dynamic loads which can lead to fatigue and structural failure of blades. Dynamic stall is one of the most studied phenomena experienced by helicopter rotors and remains a challenging issue for numerical simulation since it involves several mechanisms which are not well understood and difficult to predict.

This paper intends to demonstrate that the elsA software contains accurate and robust numerical and modelling features to address all these topics. The main capabilities of elsA [1] are recalled in section 2. Section 3 highlights recent numerical studies performed at ONERA for a wide range of challenging aerodynamics applications. These are classified in five paragraphs. Paragraph 3.2 is related to applications needing different meshing strategies, the next

DOI: 10.13009/EUCASS2019-434

one deals with turbulence and transition modelling and the following paragraph applies to unsteady flows either due to relative motion or due to turbulence properties. Paragraph 3.5 provides examples of elsA aeroelastic computations and the following one illustrates the ability of elsA to deal with stall phenomenon. Finally perspectives and current work of prime importance is quickly presented in section 4.

2. General description of the elsA CFD software

For about 20 years, the elsA software is simultaneously a basis for CFD research, a software package capitalizing on the innovative results of research over time, a tool allowing investigation and understanding of flow physics, and a multipurpose tool for applied CFD and multi-physics [1][32]. The range of aerospace applications covered by elsA is very wide: aircraft [33][30], helicopters [34], tilt-rotors [35], turbomachinery [6][36], wind turbines [37], missiles, unmanned aerial vehicles, launchers… For turbomachinery, all types of multi-stage axial, radial or mixed-flow configurations are addressed: compressors [25][26][27], turbines [28], fans [29][7], propellers or contra-rotating rotors [31].

First, let us recall the main features of the elsA multi-application CFD simulation software. This software deals with internal and external aerodynamics from the low subsonic to the high supersonic flow regime and relies on the solving of the compressible 3-D Navier-Stokes equations.

elsA allows for the simulation of the flow around moving deformable bodies in absolute or relative frames. A large variety of turbulence models from eddy viscosity to full DRSM are implemented for the RANS equations [38][39]. We can mention numerous one- or two-equation turbulence models (Spalart-Allmaras, k-ω and k-ε families, k-l Smith models…), more advanced ones, such as the non-eddy viscosity EARSM [39] and several versions for the DRSM, as well as the SAS approach which is available in elsA for k-ω and DRSM models [40][27]. Various laminar-turbulent transition modelling exist in elsA to address natural or by-pass transition [38]. The approaches that have initially been implemented rely either on local or non-local criteria, or on solving additional transport equations as the Menter-Langtry [41][42]. Then developments around criteria have enabled the increase of the Mach domain application [43] and also a huge simplification for the user (criteria transition model written under transport equations formalism). As for the Menter-Langtry model, several correlation functions are available included some developed at ONERA [44] and taking into account roughness is now possible [28]. A database approach for natural transition prediction [45] also called Parabola method, as well as a new laminar kinetic energy model [46] for bypass transition have also been implemented and tested in elsA. Various approaches for DES [47][48][30] and LES are also available.

Complex geometrical configurations may be handled using highly flexible techniques involving multi-block structured body-fitted meshes: these techniques include patched grid and overset capabilities (Chimera technique) [49][50][51][33][36]. From this initial multi-block structured meshing paradigm, elsA has evolved toward a quite complete multiple gridding paradigm including the local use of unstructured grids [52][25] in some blocks of a multi-block configuration, as well as adaptive Cartesian grids [49][50][53].

The system of equations is solved using a cell centered finite-volume method. Space discretization schemes include classical second order centered or upwind schemes and higher order schemes. The mostly used integration of the semi-discrete equations relies on a backward Euler technique with implicit schemes solved by robust LU relaxation methods. The convergence is accelerated by the use of multigrid techniques for steady flows. The implicit Dual Time Stepping method or the Gear scheme is employed for time accurate computations. elsA also includes an aeroelastic subsystem [54][31] which gives access in a unified formulation to various types of aeroelastic simulations. The simulation types range from non-linear and linearized harmonic forced motion computations, to static coupling and consistent dynamic coupling simulations in the time-domain, with different levels of structural modelling (“reduced flexibility matrix” for static coupling, modal approach, or full finite element structural model). The elsA software offers also a framework for optimization design thanks to its optimization module for the calculation of sensitivities by linearized equation solution or by adjoint solver techniques [55][56][3][23][24].

The elsA platform refers to elsA solver and several pre and post-processing Python modules, such as Cassiopée [51], used in particular for transforming input data, for Chimera pre-processing, post-processing… elsA is based on an OO design method and is coded in three programming languages: C++ as the main language for implementing the OO design, Fortran for implementing time-costly scientific computation methods, and the Python interpreted OO language for the user interface. The CGNS/Python mapping of the CGNS/SIDS is used for interoperability and coupling with elsA. The software has been ported to most HPC platforms, achieving good CPU efficiency on both scalar multi-core computers and vector computers [14].

A list of more than 130 references based on elsA in peer-reviewed journals is available at http://elsa.onera.fr/publications.html .

DOI: 10.13009/EUCASS2019-434

3. Recent challenging studies

3.1 Preambule

The reader must refer to the main references mentioned in each following subsection in order to obtain more details on the computed configurations, the meshing and numerical steps, as well as a deeper interpretation of the results and their comparison to experiments when appropriate. In the current paper, only main conclusions are provided.

3.2 Different meshing strategies in elsA software

Chimera technique for drag analyses of the Common Research Model Airliner in DPW-6

The paper [57] describes the CFD studies carried out at ONERA with elsA in the framework of the Sixth AIAA Drag Prediction Workshop. Different configurations of the well-known Common Research Model have been used to perform drag analyses and increment assessments. The structured overset grids provided by The Boeing Company to the DPW community have been preprocessed with the in-house software Cassiopée [51]: CGNS conversion, cell blanking, and overlapping issues have been handled before running these grids with the RANS solver elsA and the ONERA far-field code ffd72. Contrary to the original CRM configuration used in DPW-5, the wing shape is now based on wind-tunnel aeroelastic measurements: through a grid convergence process, a four-count drag increment between new and former wing–body geometries has been quantified, which is very consistent with previous ONERA results. Then, a CRM configuration including a throughflow nacelle–pylon installation has been computed: the corresponding drag increment of about 22 counts is in very close agreement with NASA's experimental data. Finally, horizontal and vertical tails have been added to the wing–body–nacelle–pylon geometry so that the aerodynamic performance of such a complete cruise configuration can be assessed.

Figure 1 : Complete configuration; Ma=0.85, Re= 5 millions, and CL=0.5; pressure field on suction side.

Hybrid structured/non structured grid strategy for the modelling of technological effects on a multi-row film-cooled turbine blade

As already mentioned technological effects present in turbomachinery configurations must be taken into account in numerical computations. Such geometrical details, characterized by their small dimension, can be addressed with elsA with a multi-block structured approach using the Chimera technique which offers flexibility in the grid generation. Yet the main drawback of the Chimera method is that it induces local conservation losses, leading to uncertainties on the evaluation of the massflow which is a key parameter in turbomachinery applications. Paper [25] deals with an alternative grid approach, based on the use of hybrid structured/non structured grids. The main principle of the grid approach is to mix within the computational domain structured and non structured zones which are connected with conformal matching frontiers in order to be conservative. Both structured and unstructured grids are generated separately (precision and efficiency for the structured part, flexibility for the meshing of complex geometries with unstructured elements). Two complex configurations are studied. The first case is a multi-row film-cooled nozzle guide vane, and the second is a multistage compressor configuration including labyrinth seals.

The application is a film-cooled turbine nozzle guide (Figure 2 -left). This highly film cooled NGV, composed of 113 holes distributed along 10 rows, is representative of an advanced industrial turbine blade. The Chimera approach has already been used on this configuration [36]. In the current work one investigates the hybrid grid strategy illustrated on Figure 2 (right). It allows for the meshing of the cooling holes with unstructured elements, keeping structured elements in the main channel flow.

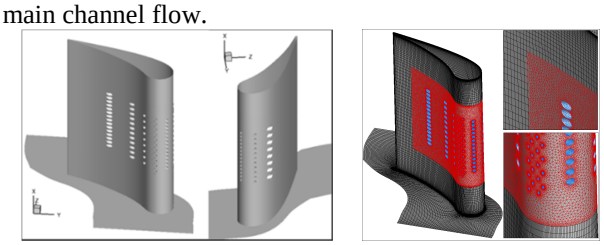

DOI: 10.13009/EUCASS2019-434

Figure 2: 3D view of the EPFL configuration (left) – Hybrid grid (right)

Such grid strategy enables to simulate the film-cooling interaction between the main channel flow and the cooling flow as illustrated hereafter. Figure 3 (left) represents a mid-span view of the Mach number distribution: as expected the main flow is deviated and accelerates within the nozzle guide vane passage. The total temperature field on the blade and on a mid-span slice represented in Figure 3 (center) exhibits qualitative satisfactory behavior: the convection of the coolant flow leaking on the blade surface and then in the blade channel. The wall heat transfer coefficient values can be computed and compared to available experimental data. Figure 3 (right) represents the heat transfer distribution obtained using three turbulence models: Spalart-Allmaras, (k-l) of Smith, and (k-ω) of Wilcox for the experimental point corresponding to an injected coolant mass flow of 10.33 g/s. One can notice that qualitatively the computations reproduce a satisfactory agreement with the experimental results.

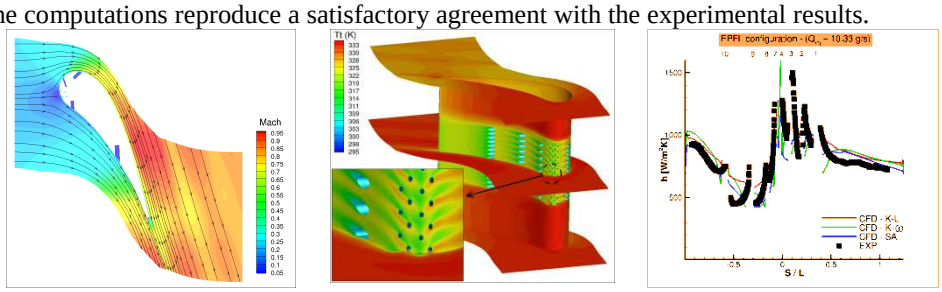

Figure 3: Mach number distribution at mid-span (left) – Total temperature field on the blade and on a mid-span slice (center) - Heat transfer distribution (right)

Let's mention that the hybrid approach developed in elsA is not restricted to the use of meshes with unstructured grids confined in small zones. The hybrid mesh can be general.

Body-Forces and Actuator Disk approaches compared to full 360° computation for fan performance in short intake nacelle

The aim of this numerical study [29] is to demonstrate that elsA is able to assess the strong aerodynamic interactions between the secondary fan/OGV stage with the airframe engine integration system and to determine if intake/fan interactions prevent the use of simplified methods which are available in the software. This study has been conducted in the frame of the European ASPIRE project (in collaboration with Airbus, DLR and NLR).

Several numerical methods have been tested. They range from RANS computations where the engine is modelled using simplified boundary conditions to full 360° URANS computations including the rotating fan blades. Intermediate methods such as Body-Forces (BD) and Actuator Disk (AD) approaches have also been assessed. The configuration studied is a double-flux isolated nacelle including a UHBR engine (fan/OGV stage). In order to obtain comparable and relevant results, a special mesh procedure is set-up to study the different fan modelling approaches (multi-block structured meshes): (i) the nacelle is meshed independently; (ii) the fan stage zone is left empty to be filled with a specific mesh for each case. Figure 4 shows the nacelle with the 2 AD (the first AD models the fan and a second AD models the OGV), the nacelle with the two Body-Force volumes at the fan (front red volume) and OGV (rear red volume) blades locations and the complete 360° case which includes all engine components (fan, OGV, core, nacelle and nozzle).

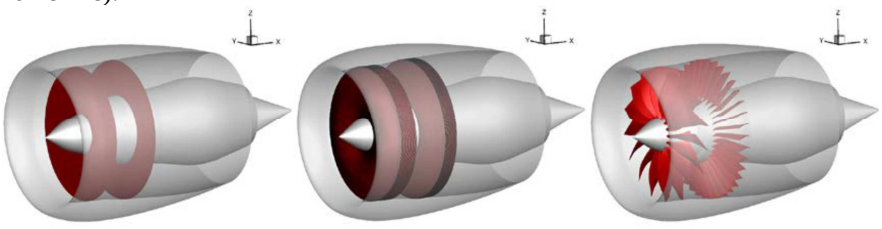

Figure 4: Visualization of the three tested approaches: (a) nacelle with Actuator Disk; (b) nacelle with Body-Forces; (c) nacelle with all fan and OGV blades.

The purpose of using the AD approach is to reduce computational time as required in a pre-design stage, while having a realistic modelling of the fan stage. The BF method consists in applying source terms to the RANS equations to model the effect of blades. In this study, the BF method is used to model the fan and the OGV blades. For RANS 360° computations, a mixing plane boundary condition is applied at the three interfaces (between nacelle and fan domains in the air intake, between fan and OGV domains; between OGV and nacelle domains) and for the URANS computations, an interpolation on the sliding mesh is performed in order to take into the account the unsteady effect. To draw more relevant conclusions, a grid convergence study is performed for all methods with three grid levels. Two operating conditions are considered: transonic cruise conditions and take-off.

DOI: 10.13009/EUCASS2019-434

In terms of global values, these results have shown that in cruise conditions, all methods are able to predict the primary and secondary mass flows with a deviation lower than 0.3% with the medium and fine grids compared to the specifications provided by Airbus. Regarding the Fan Pressure Ratio (FPR), the accuracy with respect to the specifications is about 0.1% in cruise and 0.3% at low-speed. Finally regarding fan and OGV efficiencies, the fan modelling methods and the grid size have a strong impact. Indeed, with the AD and BF approaches, the deviations are between 2 and 14% compared to the reference URANS computations on the medium grid. The differences between RANS and URANS are rather small.
Radial and surface distributions of static and stagnation pressure have also been compared. Results show that among the simplified approaches only the BF model is able to capture the main tendencies regarding the radial distributions but also the distortion maps downstream of the OGV blades (Figure 5). The 360° RANS computations provide relatively accurate results for the radial distributions but cannot correctly predict the distortion maps downstream of the OGV due to the azimuthal averaging of the flow using the mixing plane boundary condition.

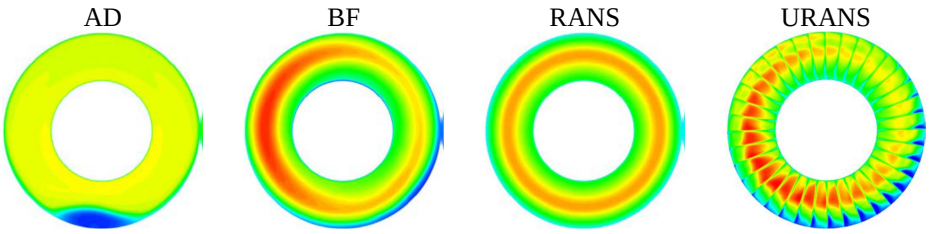

Figure 5: Stagnation Pressure maps downstream of the OGV for the different fan modelling approaches (Medium grid computations) at a low speed condition.

In conclusion, to correctly model the fan in terms of mass flow or FPR, simplified methods like the BF can provide realistic results but 360° computations are required to have a good estimation of the fan and OGV efficiencies. With high distortion levels in the air inlet, the steady RANS computations are not able to correctly transfer these distortions through the fan and OGV stages, which could be critical in off-design conditions (at low-speed or in cross-wind conditions).

RACER Aero-Acoustic Propeller Analysis and Design

ONERA work in [34] investigates the lateral rotors of the RACER, Airbus Helicopters high-speed demonstrator. These lateral rotors also defined as propellers, provide anti-torque in hover and thrust in cruise flight. The first action was to better understand the complex aerodynamic interactions that the propellers undergo in hover and cruise flight. Then, in view of optimizing the aerodynamic and particularly the acoustic performance of the propellers, their design was adapted to exploit synergistically the installation effects. Optimization included airfoil optimization and blade design, taking into account structural and manufacturing constraints. By using a smart choice of multi-fidelity simulations, ONERA improved drastically the aerodynamic and acoustic performance of the RACER.
Figure 3 (left) illustrates an URANS simulation of the RACER vehicle and its two propellers, one rotating counter to the wing tip vortex and one co-rotating, in cruise conditions provided a high-fidelity prediction of the power savings in rotating the propellers counter to the wing tip vortex instead of co-rotating. In forward flight, the main rotor can increase the efficiency of the propellers under certain circumstances. This phenomenon has been investigated using PUMA free-wake simulations. The conclusion is that the main rotor slows down the propeller axial inflow, which as a result raises propeller efficiency. For some selected configurations the rotating blades of the main rotor have been solved by CFD, whereas the propeller was accounted for via a coupling with PUMA (Figure 3-right).

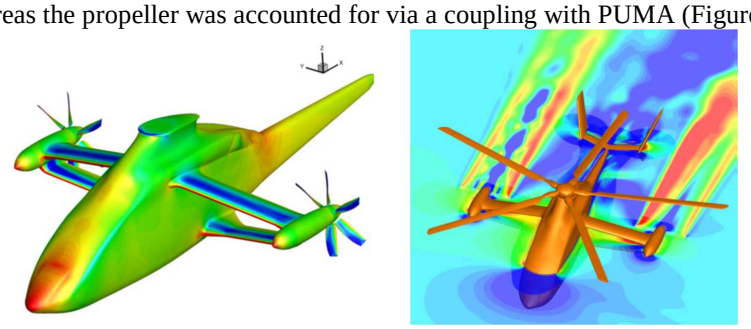

Figure 6 : elsA unsteady simulation of the RACER with propellers mounted on both sides (left) - Complete RACER with main rotor CFD simulation coupled with PUMA propellers modelling (right).

DOI: 10.13009/EUCASS2019-434

3.3 Turbulence and laminar-turbulent Transition modelling examples in elsA

Assessment of scale adaptative simulation

CFD results depend significantly on the Navier-Stokes closure i.e. on the used turbulence model and turbulence approach (RANS, DES, LES, DNS). Classically, the RANS turbulence model is based on the Boussinesq hypothesis by using a model with one or two transport equations such as the Spalart-Allmaras or the Menter SST models. The turbulence is clearly anisotropic in the vicinity of the tip gap and second moment closure DRSM is able to capture this characteristic. Zonal DES was also performed at ONERA [58][59] to study the tip leakage vortex and its interaction with incoming wakes and vortices. The SAS approach is a way to enhance traditional RANS model with low implementation effort. It can improve dramatically unsteady RANS computations especially when massive flow separation occurs, even for non refined grids. A well-known example is the jet in crossflow [40]. The classical turbulence models (even DRSM) fail reproducing the diffusion of the jet downstream, whereas the same models coupled with the SAS approach perfectly reproduce the experiments, using classical RANS grids. The standard SAS approach of Menter associated to the SST k-ω model [60] is present in elsA for years [40]. The SAS approach can be generalized to any RANS turbulence model. It has been implemented in elsA [27] for the DRSM model (only the term, responsible for the decrease of the eddy viscosity in case of occurrence of flow instabilities, has to be added to right side of the ω-scale transport equation). The study presented in [27] aims at validating this combination.

The first rotor (R1) of the axial compressor CREATE [61] is investigated. CFD setup computational domain, mesh and boundary conditions and numerical methods are detailed in [27]. Two meshes are used. This first one (M1) can be considered as a fine mesh for URANS simulation, the second grid is the same used for ZDES simulation of [58][59]. SAS-DRSM computation is compared to URANS using k-ω SST or DRSM models, as well to SAS-SST and ZDES computations, and experimental data.

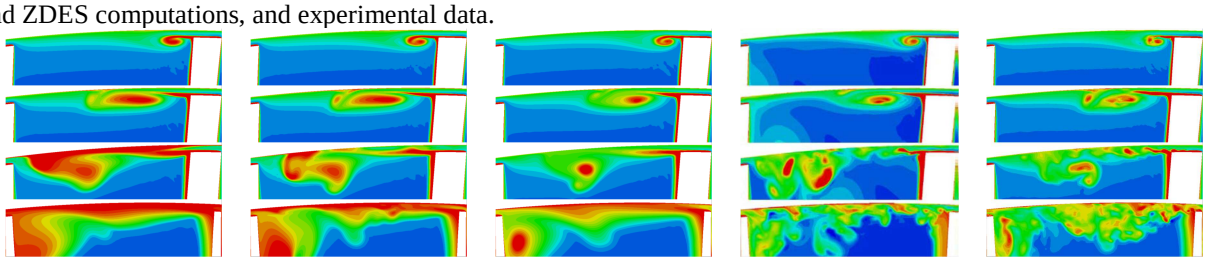

Figure 7: Instantaneous entropy fields at 22.3%, 31%, 46% and 96% x/c for (from left to right): M2-URANS-SST, M2-SAS-SST, M2-URANS-DRSM, M2-ZDES, M2-SAS-DRSM

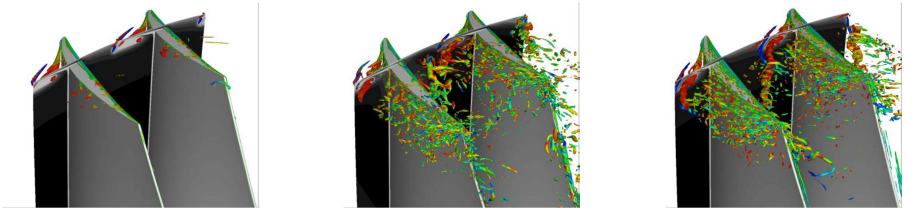

Figure 8: Instantaneous view of the tip leakage flow for (from left to right): M2-SAS-SST, M2- M2-ZDES and M2-SAS-DRSM

The instantaneous entropy variation field at four axial locations for all simulations is depicted in Figure 7, and an instantaneous view of the tip leakage flow is shown for SAS and ZDES computations in Figure 8. The SAS-DRSM approach much better captures turbulent structures than URANS/SST, URANS/DRSM, SAS-STT computations. The global representation of turbulent structures with SAS-DRSM is close to ZDES.

Reference [27] provides a full analysis of the computations by exploring the time-averaged flow in the blade passage and downstream of the rotor, as well as the time-averaged radial profiles, time-averaged overall performances and comparison to experiments. Besides, all power spectral densities (PSD) are depicted (in Figure 9).

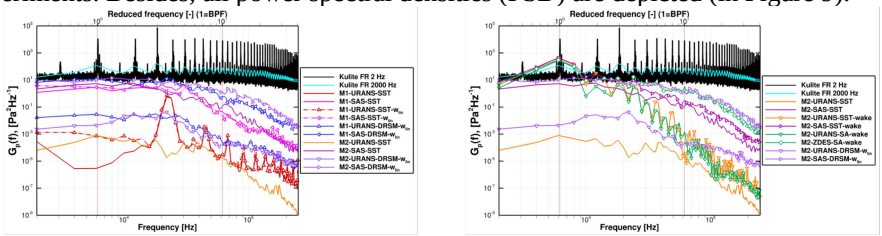

Figure 9: PSD of static pressure for all meshes (left) and only M2 mesh (right)

DOI: 10.13009/EUCASS2019-434

The comparison of the two meshes shows that with the first mesh, the SAS-DRSM technique is able to capture the same PSD as the second mesh up to the ninth harmonics (on the same mesh, the discrepancy between ZDES and SAS-DRSM arises at the 20th harmonics) while the first mesh is ten times smaller.

Stability-based transition model by means of transport equations

An implementation of the stability based on the Arnal-Habiballah-Delcourt criterion [62] by means of transport equations is presented in [63]. This criterion, valid for Mach number up to M = 4 and for heated and cold wall, is combined with C1 [64] and Gleyzes [65] criteria to account for cross-flow transition and transition in separation bubbles. The implementation by means of transport equations was validated by comparing with results obtained with the boundary layer equations solver 3C3D (ONERA code) on the M6 wing (Figure 1, a and b) and on the XRF1 nacelle (Figure 10, c and d). The method may be applied at early design stages as good agreement was observed even on poorly refined mesh generated automatically. Transition prediction close to exact local linear stability computations can be obtained thanks to the method of Bégou et al. [45] for higher computational cost. This latter method complements well with the method presented in the paper [63] as it can be used in more advanced design stages.

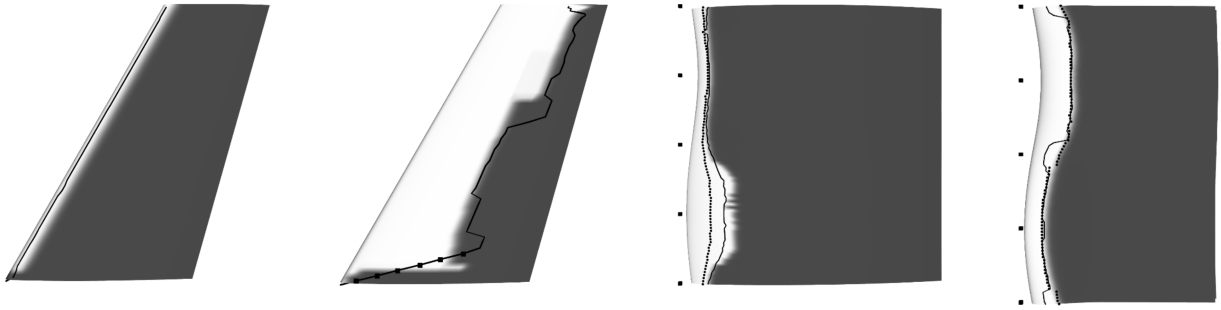

Figure 10 : Intermittency contours (light and dark corresponds respectively to = 0 and = 1) at the suction (a) and pressure (b) M6 sides (the black line depicts the transition location predicted by 3C3D by means of AHD/C1) and at the outer (c) and inner (d) sides of the XRF1 nacelle. For c and d images the black line (respectively the black symbols) depicts the transition location predicted by 3C3D by means of AHD/C1 criteria (resp. parabola method).

3.4 Selected Unsteady flow computations with elsA software

Multiple-frequency phase-Lagged approach for the computation of turbomachinery flows

The computational cost of a time-accurate full-annulus computation remains very high, despite the increase of HPC resources. It is therefore important to have access to numerical methods that reduce the computational domain and are efficient enough to simulate accurately the main unsteady effects. To alleviate the problem, the phase-lagged method is commonly used for unsteady rotor/stator simulations to reduce computing resources. This method, limited to flow configurations including a single periodic perturbation (as one single-stage or one row under vibrations), enables the computation of the periodic flow around one blade per row, using appropriate phase-shifted boundary conditions at the pitchwise boundaries. A generalization of the phase-lagged approach, called MFA allows unsteady computations through several rows, whilst still limiting the computational domain to one single blade-to-blade passage in each row is available in elsA. An evaluation of the MFA approach is presented in [26]. The first part of the paper presents the method and discusses the associated assumptions and limitations. The method is evaluated on the 3.5 stage axial compressor CREATE [61]. The CFD results are analysed and compared both with experimental data and with a elsA reference multipassage computation (RC) based on a sliding mesh approach [61]. An example of flowfield reconstruction is illustrated in Figure 11. They are compared to snapshots obtained with the RC and the mixing-plane steady computations (MPC). One can observe that the main flow structures seen in the RC computation are quite well captured by the MFA simulation.

DOI: 10.13009/EUCASS2019-434

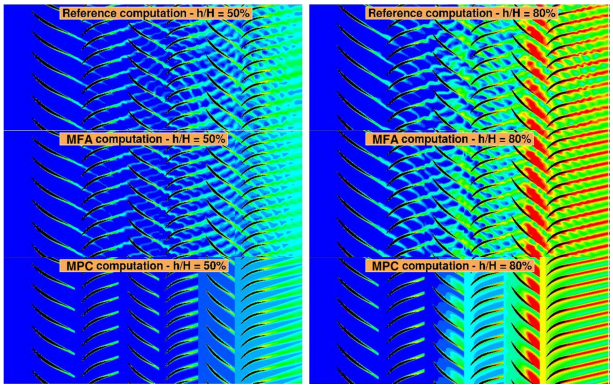

Figure 11: Entropy snapshots at h⁄H = 50% and h⁄H = 80%.

The MFA approach enables the simulation of unsteady effects on a multistage turbomachinery and access to unsteady information that would not be available with a MPC. A detailed analysis underlines the limits of the MFA. If the method is capable of capturing unsteady effects linked to the adjacent upstream and downstream blade rows passing frequency, it fails modelling clocking effects, i.e., the relative influence between rows N and N+2.

Jet noise using ZDES: external boundary layer thickness and installation effects

In order to compute accurately jet noise, reliable unsteady approaches are needed to simulate the turbulent mechanisms which generate noise. LES has proven to be efficient to do so but this approach is challenging to implement in an industrial framework when dealing with complex geometries for which it does not seem to be reasonable nor relevant to resolve the turbulence production mechanisms in all attached boundary layers (BL). Hybrid RANS/LES methods have been developed to model the attached BL (or at least the internal part) and resolve turbulence in free shear layers.

The ZDES [48] approach available in elsA for years has been used with success for different academic and technical configurations. In [30], ZDES in its automatic mode (namely mode 2, [66]) is used to simulate industrial configurations of jets (UHBR nozzle and evaluate the effect of the external BL thickness and of the wing/flap installation. Very small differences have been observed on the aerodynamic properties of the jet when increasing the nacelle external BL thickness. Figure 12 shows that the thicker external BL leads to a slightly shorter jet.

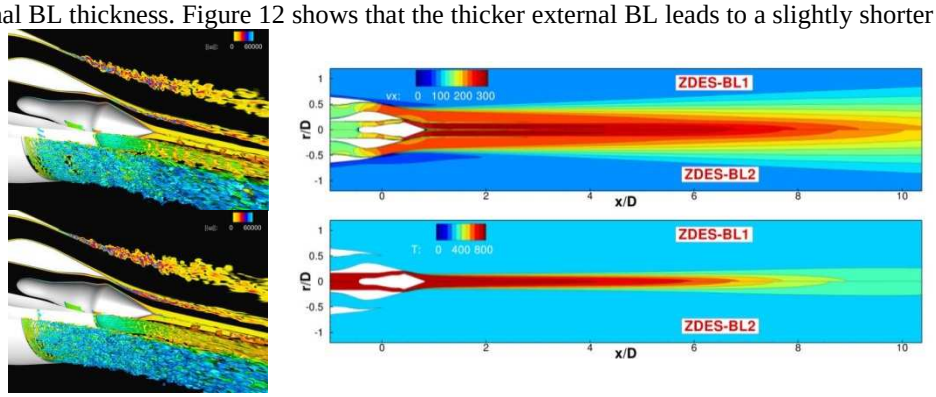

Figure 12: Q criterion isosurfaces and contours of vorticity (left) for the thin (BL1 - above) and thicker (BL2 - below) boundary layer - Streamwise velocity and static temperature fields (rigth)

An acoustic analysis is performed with the FWH approach and recent ONERA developments allowing the use of closed surfaces. At medium frequencies the results display high noise levels attributed to vortex roll-ups at the nozzle exit. The noise variation between the baseline BL case and the thick BL case varies within a range of +/- 0.5 dB. This low sensitivity of the radiated noise may be attributed to the fact that the baseline BL is already rather thick for this type of flow.

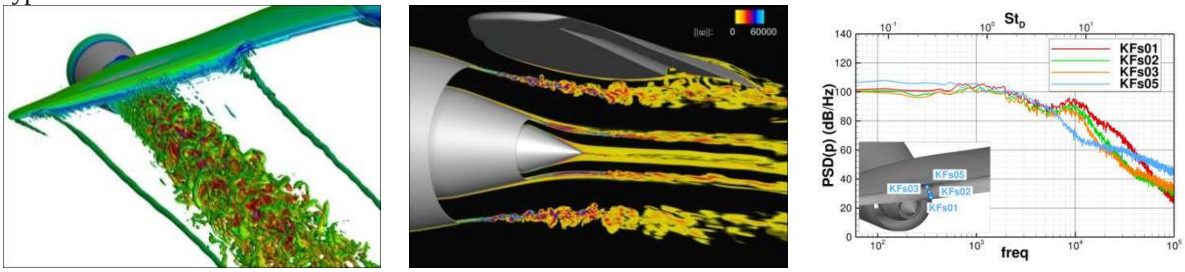

DOI: 10.13009/EUCASS2019-434

Figure 13: Q criterion isosurface colored by streamwise velocity - Norm of the vorticity (center) - Wall pressure spectra on the upper side of the flap (right)

Q criterion isosurface and norm of the vorticity are plotted in Figure 13 for the installed configuration. Regarding the installation effect it was shown that the jet length is reduced by 30% due to the presence of the wing and flap and that the mean jet direction is deviated due to the jet impinging the trailing edge of the flap (which participates to the jet length reduction). This interaction leads to some increased temperature and pressure fluctuations on the flap which creates noise sources at f = 10 kHz (Figure 13 right). The presence of the wing entails a shielding effect of the acoustic waves and the near-field fluctuating pressure levels are decreased in the direction above the wing. Work related to jet noise is currently devoted to the use of ZDES mode 3 to enable WMLES inside the nozzle and alleviate the RANS-to-LES transition related noise.

3.5 Two examples of relevant aeroelastic computations with the elsA software

Aeroelastic gust response for different critical gust shapes

Gusts encountered by airplanes induce loads that can be critical for some severe flight conditions, and therefore must be considered in the sizing in a structure design process. Furthermore, in the context of aircraft drag optimization and weight saving, airplane structures become increasingly flexible (large span, high wing aspect ratios). There is then a need to accurately assess gust loads. The paper [67] presents some recent work achieved at ONERA concerning high-fidelity simulations for gust response. First, a physical validation of the gust response simulation is performed by comparing the results to those obtained experimentally on a scaled model. Second, numerical comparisons are performed using various techniques, in order to model the gust. Finally, an application for generic regional aircraft is shown.

Coupled CFD/CSM hot shape prediction CROR and comparison with experimental data

In [31] CROR wind tunnel tests results are compared to numerical hot shape (i.e. the deformed shape due to centrifugal forces and aerodynamic loads during the flight) computations. In a previous paper numerical computations were performed using the design shape in both CFD and CSM computations. The current study is a step forward. The blade manufacturing failures (Figure 14 –center) are introduced and the finite element model is tuned considering these new shapes. The flowchart for the CFD/CSM static coupling is shown in Figure 14 (right). Once the flow has converged toward a steady solution, the aerodynamic forces and moments are extracted from the CFD grid to be interpolated on the CSM grid. This is done inside the aeroelastic interface. These structural loads are then injected in the CSM solver (©Nastran) which computes the displacements of the structure submitted to these loads. The aeroelastic interface then interpolates these displacements from CSM grid to CFD grid aeroelastic interfaces and propagates the displacement in the aerodynamic volume mesh using a mesh deformation tool. This process is continued until convergence to equilibrium between the loads and the structural displacements, using a relaxed fixed point procedure.

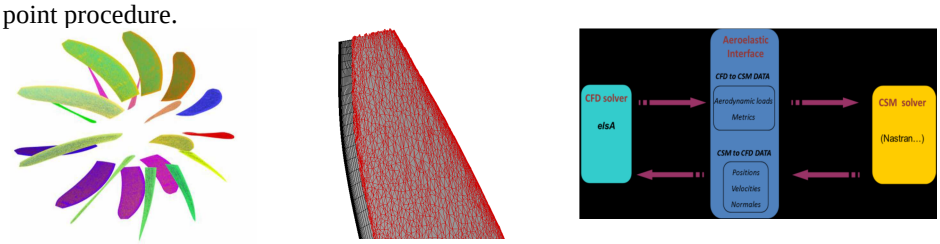

Figure 14 : Rotor blades (left) - CAD blade mesh surface in black and manufactured blade mesh surface in red (center) - Static coupling strategy elsA/Nastran (right)

Then, blade displacements and blade pressure distributions are compared. If some differences are still noticeable concerning the blade displacements, this methodology improved a lot the blade pressure distributions correlations with the experimental data.

These encouraging results show that manufacturing failures can have a non-negligible impact on the numerical / experimental comparison and must be evaluated and, if necessary, be taken into account.

3.6 Stall phenomenon computation with elsA software

Numerical Analysis of RPM effect on Dynamic Stall on Helicopter Rotor at Forward Flight -

Dynamic stall is a highly complex phenomenon characterized by unsteady massive separated flow. It limits the flight envelope of helicopters by generating vibrations and large dynamic loads which can lead to fatigue and structural failure of blades. Dynamic stall involves several mechanisms which make the numerical prediction of stall difficult

DOI: 10.13009/EUCASS2019-434

and the understanding of the phenomenon still incomplete. In [68] a loose coupling methodology between CFD code elsA and a Comprehensive Analysis code is used to simulate the problem. Airbus Helicopter HOST code is used to take into account the blade motion and deformation. Three stalled flight conditions have been selected in the wind tunnel 7A rotor test data to investigate the revolution per minute (RPM) effect on the dynamic stall onset and the related mechanisms. The model-scale 7A rotor is shown on Figure 15 in the transonic closed circuit S1MA wind tunnel at ONERA Modane test center, France. Figure 15 also shows the mesh (Chimera background grid, blade mesh, rotor and test stand surface mesh). For all cases, the numerical simulations have shown satisfactory agreement with the experimental data with regard to trim parameters (less than 0.3 deg difference with experiment for all control angles), airloads and structural loads (dynamic stall events correctly predicted in magnitude and phase). Different stall events have been distinguished for each case. The stall intensity increases with the decrease in the RPM. A trailing edge stall is observed for all cases in the inner part of the blade. For the two highest RPM cases, the blade tip undergoes one stall event at the beginning of the fourth quadrant of the rotor disk while it sees a double stall in the fourth quadrant for the lowest RPM case. The mechanisms which lead to these different stall events have been deeply investigated in this work. The onset of stall has been associated to the impact of the tip vortex generated by the other blades. The trailing edge stall and the strong leading edge stall occurring at the blade tip are triggered by the angle of attack induced by the vortex passing close to the blade (Figure 15, rigth). Stall only occurs when the kinematic induced angle of attack added to the vortex induced angle of attack is high enough. The second stall event in the low RPM case is connected to a second blade-vortex interaction. It takes place when the blade meets the tip vortex coming from the previous blade.

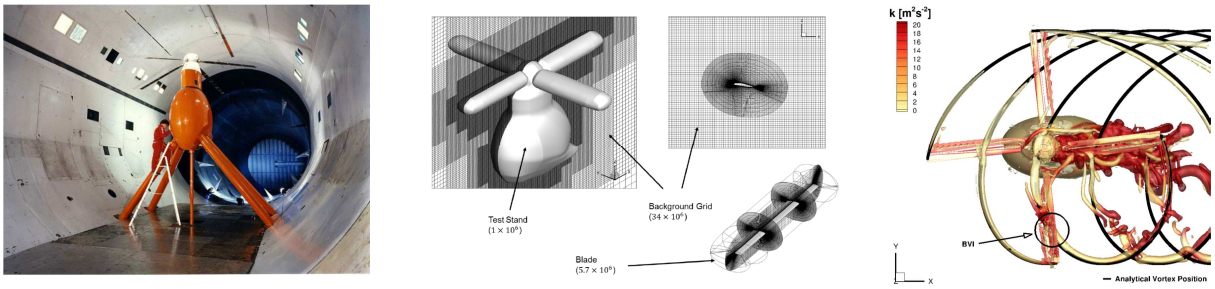

Figure 15 : 7A rotor mounted in S1MA Wind Tunnel - Overset Structured mesh - Analytical tip vortex and isocontour of Q-criterion colored by the turbulent kinetic energy

Active flow control at the engine/wing junction on a realistic high-lift aircraft configuration

The purpose of the activities presented in [69] is to assess the potential of active flow control system to delay and contain the nacelle wake separation that eventually appears on the wing suction side at high angles of attack on a realistic high-lift aircraft configuration including slats and flap deployed for landing conditions as well qas a HBR engine. ONERA has performed this study in the framework of the European Project AFLoNext. Overset structured and grids have been built (Figure 16). For the baseline configuration with-out flow control, the maximum lift coefficient CL_{max} and the angle of attack at which the massive flow separation appears (stall behavior) were determined and the flow patterns, especially the emerging vortices from pylon, slats, and strake, were studied. Following this work, several Active Flow Control (AFC) systems and settings were defined and evaluated, at first with RANS computations. Different slot sizes and types (continuous vs. segmented, see Figure 16, left) and/or blowing ve-locities were proposed. The potential of each system was shown over a whole polar in comparison with the baseline. The Figure 17 gives the C_{fx} distribution and friction lines at an incidence of 16 ° for baseline and devices n◦2, 4, and 6.The gain that is obtained with an AFC system is consistent with its C_μ coefficient value which represents the actuation force over the flow: a greater C_μ leads to more significant gains. In constant blowing mode, all the AFC systems assessed in this study produce lift level gains after stall (typically about +5%). It was demonstrated that for C_μ values compatible with aircraft manufacturer requirements, a constant blowing AFC system is efficient to delay and contain the massive flow separation which extends downstream of the engine/wing junction without control: the wing stall can be delayed of 1 to 2◦ of angle of attack with the considered devices and settings, and it can also be smoothed and the CL_{max} can be slightly increased (1 to 3%).

As a last step, URANS computations have been performed to assess the potential gain of a pulsed jet actuator. The 14-slot sys-tem, which is probably the device the most representative of what may be tested in future AFLoNext wind tunnel tests, was evaluated with each slot blowing out of phase with its neighbours. The baseline without control has also been computed as a reference point in URANS. The gain obtained with the pulsed blowing system is similar (Figure 18) to the one of constant blowing devices that have greater C_μ and mass flow rate values, which seems to confirm that this type of AFC approach can be promising.

DOI: 10.13009/EUCASS2019-434

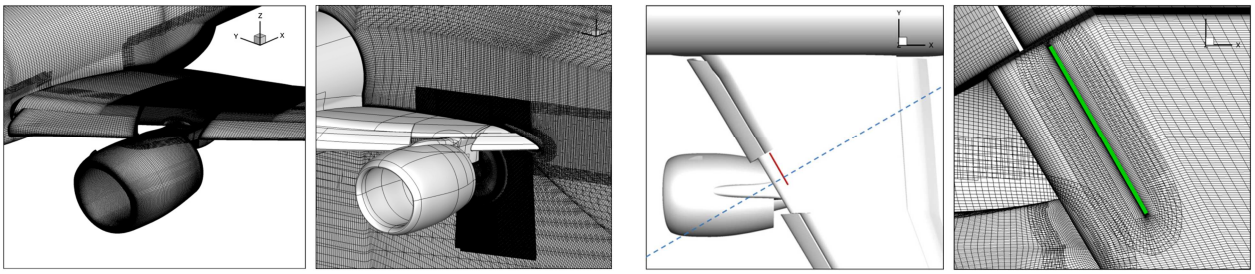

Figure 16: Structured grids on aircraft surfaces and refinement boxes in areas of interest (two left figures) – Position and initial grid of AFC systems (two right figures).

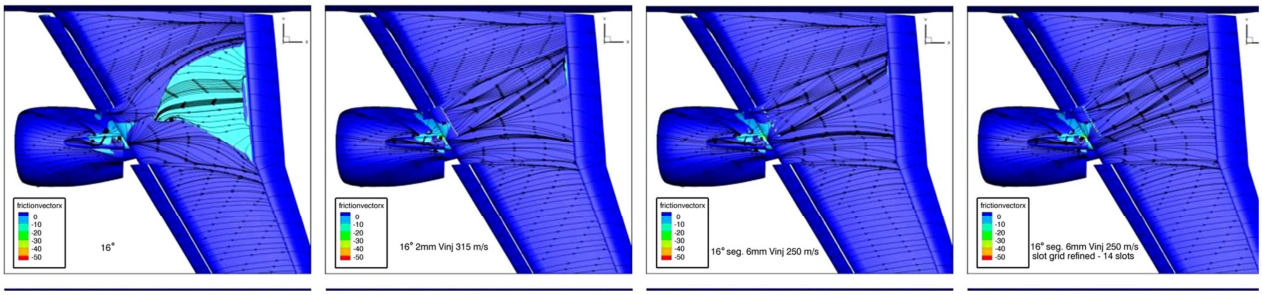

Figure 17: C_{fx} distribution and friction lines at an incidence of 16 ° for baseline and devices n◦2, 4, and 6.

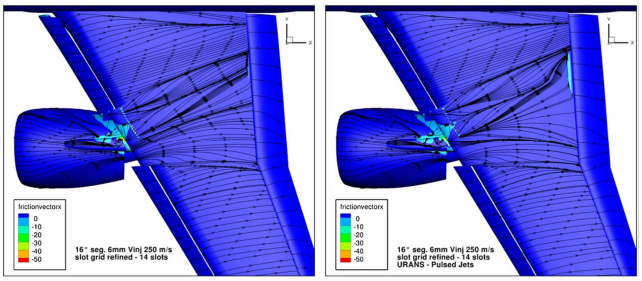

Figure 18: C_{fx} distribution and friction lines at 16◦; 14-slot device RANS (constant) vs. URANS (pulsed).

4. Conclusion and Perspectives

The previous section has presented recent very challenging aerodynamics studies. That demonstrates that the elsA software has become a very mature and reliable tool for CFD studies, which can be used for industrial design and for advanced research in aircraft, helicopter and turbomachinery field.
An important work which revolutionizes the architecture of the software is in progress. The first results in terms of CPU provide very important gains (ensuring exactly the same numerical solution as with the former architecture). One of the test cases is a stage of the CREATE axial compressor presented above. For a RANS computation with Spalart-Allmaras model the CPU gains range from a factor of 3 in structured mesh to a factor of 6 with an unstructured mesh. The elsA V4.0 release produced in 2018 already contains these achievements for a limited scope of the numerical and modelling parameters present in elsA. Details will be published shortly by the elsA team.

Acknowledgments

The studies presented in this paper are making use of the elsA-ONERA software, whose the co-owners are Airbus, Safran, and ONERA. Since 2015, the development and validation of the elsA software are driven by a close research and financial cooperation, as well as a common governance, between ONERA, Airbus and Safran groups.
The author wants to acknowledge all the people which have carried out the simulations whose results are presented in this paper: H. Bézard, A. Burlot, C. Castells, L. Castillon, M. Costes, J. Dandois, G. Delattre, S. Dequand, C. François, H. Gaible, F. Gand, D. Hue, F. Huvelin, A. Lepage, C. Liauzun, J. Marty, B. Maugars, M. Méheut, B. Michel, L. Pascal, T. Renaud, F. Richez, I. Salah El Din, F. Sartor, M. Soismier, M. Vergez.
The author would like also to thank all who have made the elsA software project so successful for many years.

DOI: 10.13009/EUCASS2019-434

References

[1] L. Cambier, S. Heib, and S. Plot. "The Onera elsA CFD software: input from research and feedback from industry". *Mechanics & Industry*, 14(3):159–174, 2013.

[2] W. Thollet, G. Dufour, X. Carbonneau, F. Blanc, "Body-force modeling for aerodynamic analysis of air intake – fan interactions", September 2016, *International Journal of Numerical Methods for Heat and Fluid Flow* 26(7):2048-2065.

[3] G. Carrier, D. Destarac,A. Dumont, M. Méheut, I. Salah El Din, J. Peter and S. Ben Khelil, J. Brezillon, M. Pestana, "Gradient-Based Aerodynamic Optimization with the elsA Software", *52nd Aerospace Sciences Meeting - AIAA SciTech 2014*, National Harbor, Maryland· January 2014.

[4] van der Wall, B.; Kessler, C.; Delrieux, Y.; Beaumier, P.; Gervais, M.; Hirsch, J-F.; Pengel, K.; Crozier, P., "From Aeroacoustics Basic Research to a Modern Low-Noise Rotor Blade", *Journal of the American Helicopter Society*, Volume 62, Number 4, October 2017, pp. 1-16(16)

[5] Léon, E. R.; Le Pape, A.; Costes, M.; Désidéri, J.-A.; Alfano, D., "Concurrent Aerodynamic Optimization of Rotor Blades Using a Nash Game Method", *Journal of the American Helicopter Society*, Volume 61, Number 2, April 2016, pp. 1-13(13)

[6] D. Guegan, M. Schvallinger, F. Julienne, N. Gourdain, and M. Gazaix. "Three-dimensional Full Annulus Unsteady RANS Simulation of an Integrated Propulsion System", *51st AIAA/SAE/ASEE Joint Propulsion Conference, AIAA Propulsion and Energy Forum*, AIAA 2015-4021.

[7] T. Berthelon, A. Dugeai, J. Langridge, F. Thouverez, "Ground Effect on Fan Forced Response, *Proc. of the 15th International Symposium on Unsteady Aerodynamics, Aeroacoustics & Aeroelasticity of Turbomachines*, 2018, ISUAAAT15-094

[8] F. Blondel, M. Stanciu, F. Leboeuf, M. Lance, " Modeling Unsteadinesses and Polydispersion in wet steam flows using the quadrature method of moments and a two-equation model", *10th European Conference on Turbomachinery Fluid dynamics & Thermodynamics*, April 15-19, 2013, Lappeenranta, Finland.

[9] Stanciu, M., Marcelet, M., Dorey, J.M., "Numerical Investigation of Condenser Pressure Effect on Last Stage Operation of Low Pressure Wet Steam Turbines", *Conference: ASME Turbo Expo 2013: Turbine Technical Conference and Exposition*, June 2013.

[10] G. Dufour, F. Sicot, G. Puigt, C. Liauzun, A. Dugeai, "Oscillating-Flap Simulations with the Time-Spectral and Linearized Methods", *AIAA Journal* 48(4):788- 797, April 2010.

[11] F. Sicot, G. Dufour, N. Gourdain, "A time-domain harmonic balance method for rotor/stator interactions", *J. of Turbomachinery*, 134(1):011001 (13 pp.), 2012.

[12] Y. Colin, H. Deniau, J.-F. Boussuge, "A robust low speed preconditioning formulation for viscous flow computations", *Computers and Fluids*, 47(1):1-15, 2011

[13] S. Le Bras, H. Deniau, C. Bogey, G. Daviller, "Development of Compressible Large-Eddy Simulations Combining High-Order Schemes and Wall Modeling", *AIAA Journal* Vol. 55, No. 4, pp. 1152-1163, Avril 2017

[14] N. Gourdain, M. Montagnac, F. Wlassow and M. Gazaix, "High-performance Computing to Simulate Large-scale Industrial Flows in Multistage Compressors". *Int. Journal of High Performance Computing Applications*, vol. 24, 2010.

[15] G. Després, G. Ngo Boum, F. Leboeuf, D. Chalet, P. Chesse, A. Lefebvre, "Simulation of near surge instabilities onset in a turbocharger compressor" - *Proc. of the Inst. Mech. Eng., Part A, J. of Power Energy* 227, 665–673, 2013.

[16] P. Gougeon, G. Ngo Boum, "Aerodynamic interactions between a high-pressure turbine and the first low-pressure stator", *J. of Turbomach.* 136, 071010 (11 pages), 2014.

[17] Cadel A, Ngo Boum G, Thouverez F, Dugeai A, Parent M. "Computing Fluid Structure Interaction Coupling Time Spectral Method and Harmonic Balance Method", *ASME Turbo Expo 2017: Turbo. Technical Conference and Exposition*, Volume 7B: Structures and Dynamics, Charlotte, NC, USA, June, 2017

[18] I Leplot, M Leborgne, R Schnell, J Yin, G. Delattre, F. Falissard, J Talbotec, "Aero-mechanical optimization of a contra-rotating open rotor and assessment of its aerodynamic and acoustic characteristics", *9th ETC*, Istanbul , mars 2011

[19] M. Mesbah, J.-F. Thomas, F. Thirifay, R. Viguié, F. Durieu, V. Iliopoulou, O. De Vriendt, "Investigation of compressor blade vibrations due to subharmonic aerodynamic excitations", *13th Int. Symp. on Unsteady Aerodynamics, Aeroacoustics and Aeroelasticity of Turbomachines*, Tokyo, 2012.

[20] J. Babajee, T. Arts, "Investigation of the laminar separation-induced transition with the γ-$Re_{\theta t}$ transition model on one very high-lift low-pressure turbine (T2) and one engine-like scale low-pressure turbine (TX) rotor blades at steady conditions and freestream turbulence", *47th 3AF Int. Symp. of Applied Aerodynamics*, Paris, 2012.

[21] Dufour, G., Carbonneau, X., Thollet, W., Blanc, F, "Body-force modeling for aerodynamic analysis of air intake – fan interactions", *International Journal of Numerical Methods for Heat & Fluid Flow* (2016), 2048, 26

DOI: 10.13009/EUCASS2019-434

[22] A. Lerat, P. Cinnella, B. Michel, F. Falissard, “High order residual-based compact schemes for aerodynamics and aeroacoustics”, *Computers & Fluids*, Vol. 61, pp. 31-38, 2012
[23] Guénot, D. ; Gallard, F. ; Brezillon, J. ; Mérillac, Y., ”Aerodynamic optimization of a parametrized engine pylon on a mission path using the adjoint method”, June 2018, *ECCM-ECFD Conference 2018*, Glasgow, UK
[24] K. Jovanov, R. De Breuker, M. Abdalla, and C. Blondeau. "A linear aerodynamics-based preconditioner for high-fidelity aeroelastic analysis and sensitivity analysis", *17th AIAA/ISSMO Multidisciplinary Analysis and Optimization Conference*, AIAA AVIATION Forum, AIAA 2016-4123
[25] L. Castillon, M. Soismier, M.C. Le Pape, B. Maugars, B. Michel, "A hybrid structured/unstructured grid strategy for the CFD modeling of technological effects on complex turbomachinery applications", *ISABE-2019-24009 Submitted*
[26] Castillon, L., Gourdain, N., and Ottavy, X., "Multiple-Frequency Phase-Lagged Unsteady Simulations of Experimental Axial Compressor", *J. of Propulsion and Power*, (2015), accessed January 06, 2015, volume 31, issue 1 on pages 444-455.
[27] Marty, J., Gaible, H., Bézard, H., “Assessment of Scale Adaptative Simulation of a Rotor of High Pressure Compressor”, *Proceedings of ASME Turbo Expo 2018*, GT 2018, June 5-11, 2018, Oslo, Norway
[28] Minot, A., Marty, J., Perraud J. Casalis G., “Implementation of a surface roughness-based transition onset correction in the Menter-Langtry transition model”. *ASME Turbo Expo 2017*, GT2017-63237, June, 2017, Charlotte, NC
[29] A. Burlot, F. Sartor, M. Vergez, M. Méheut, R. Barrier, “Method comparison for fan performance in short intake nacelle”, *Applied Aerodynamics Conference, AIAA AVIATION Forum*, AIAA 2018-4204
[30] F. Gand, M. Huet, T. Le Garrec and F. Cléro, « Jet noise of a UHBR nozzle using ZDES: external boundary layer thickness and installation effects, *in AIAA AVIATION Forum, 23rd AIAA/CEAS Aeroacoustics Conference*, AIAA-2017-3526, 5-9 June 2017, Denver, Colorado.
[31] Mauffrey, Y., Geeraert, A., Verley, S., “Comparison between coupled CFD/CSM hot shape prediction and AIPX-7 CROR experimental data”, AIAA Paper No 2017-3915, *35th AIAA Applied Aerodynamics Conference*, Denver, Colorado, 2017.
[32] L. Cambier, M. Gazaix, S. Heib, S. Plot, M. Poinot, J.-P. Veuillot, J.-F. Boussuge, M. Montagnac, “An Overview of the Multi-Purpose elsA Flow Solver”, *Aerospace Lab*, Issue 2, 2011.
[33] D Hue, S Péron, L Wiart, O Atinault, E Gournay, P Raud, C Benoit, J. Mayeur, "Validation of a near-body and off-body grid partitioning methodology for aircraft aerodynamic performance prediction", *Computers & Fluids* vol. 117, pp. 196-211, 2015.
[34] C. Lienard, I. Salah El Din, T. Renaud, R. Fukari “RACER high-speed demonstrator: Rotor and rotor-head wake interactions with tail unit”, *American Helicopter Society*, 74th Annual Forum, Phoenix, Arizona, May 14-17, 2018
[35] J. Decours, P. Beaumier, W. Khier, T. Kneisch, M. Valentini, L. Vigevano, “Experimental Validation of Tilt-Rotor Aerodynamic Predictions”, *40th European Rotorcraft Forum*, September 2-5 2014, Southampton, U.K.
[36] L. Castillon; G. Billonnet; J. Riou; S. Péron; C. Benoit, "A Technological Effect Modeling on Complex Turbomachinery Applications With an Overset Grid Numerical Method", *Journal of Turbomachinery* , October 2014; 136(10):101005-101005-11.
[37] C. Lienard, R. Boisard, and C. Daudin, "Aerodynamic behavior of a floating offshore wind turbine", *AIAA Scitech 2019 Forum*, AIAA 2019-1575.
[38] B. Aupoix, D. Arnal, H. Bézard, B. Chaouat, F. Chedevergne, S. Deck, V. Gleize, P. Grenard, E. Laroche, “Turbulence and transition modeling”, *Aerospace Lab*, Issue 2, 2011.
[39] H. Bézard, T. Daris, “Calibrating the Length Scale Equation with an Explicit Algebraic Reynolds Stress Constitutive Relation”, *6th Int. Symp. on Engineering Turbulence Modelling and Measurements*, W. Rodi and M. Mulas editors, Elsevier, pp. 77-86, 2005.
[40] Duda, B. M., Menter, F. R., Esteve, M.-J., Hansen, T., Deck, S., and Bézard, H., “Numerical investigations on a hot jet in cross flow using scale-resolving simulations”. *7th Int. Symposium on Turbulence and Shear Flow Phenomena*, 2011.
[41] Langtry, R. B., and Menter, F. R., “Correlation-Based Transition Modeling for Unstructured Parallelized Computational Fluid Dynamics Codes”, *AIAA Journal, 2009*, 47(12), Dec., pp. 2894–2906.
[42] Benyahia, A., Castillon, L., and Houdeville, R., “Prediction of separation-induced transition on high lift low pressure turbine blade”. *In ASME 2011 Turbo Expo: Turbine Technical Conference and Exposition*, pp. 1835–1846.
[43] J. Perraud, A. Durant, “ Stability-Based Mach Zero to Four Longitudinal Transition Prediction Criterion”, *Journal of Spacecraft and Rockets*, Vol. 53, No 4, pp. 730-742, 2016.
[44] Content, C., and Houdeville, R., “Application of the γ-$Re_{\theta t}$ laminar-turbulent transition model in Navier-Stokes computations”. *AIAA, 40th Fluid Dynamics Conference and Exhibit*, 2010-4445, June 2010.

DOI: 10.13009/EUCASS2019-434

[45] G. Bégou, H. Deniau, O. Vermeersch, G. Casalis, "Database Approach for Laminar-Turbulent Transition Prediction: Navier-Stokes Compatible Reformulation", *AIAA Journal*, Vol. 55, No. 11 (2017), pp. 3648-3660.
[46] L. Jecker, O. Vermeersch, H. Deniau, G. Casalis, E. Croner, "A New Laminar Kinetic Energy Model for RANS Simulations of Bypass Transition", *AIAA Aviation forum 2017*, Denver, U.S.A, 05-09 Juin 2017.
[47] S. Deck, "Zonal-Detached Eddy Simulation of the Flow over a High-Lift Configuration", *AIAA Journal*, Vol. 43, pp. 2372-2384, 2005.
[48] S. Deck, "Recent improvements of the Zonal Detached Eddy Simulation formulation", *Theoretical and Computational Fluid Dynamics*, Vol. 26, Issue 6, pp 523-550, 2012.
[49] T. Renaud, M. Costes, S. Péron, "Computation of GOAHEAD configuration with Chimera assembly", *Aerospace Science and Technology*, Vol. 19, Issue 1, pp. 50–57, 2012.
[50] S. Péron, C. Benoit, "Automatic off-body overset adaptive Cartesian mesh method based on an octree approach", *Journal of Computational Physics*, Vol. 232, Issue 1, pp. 153–173, 2013.
[51] Benoit, B., Péron, S., and Landier, S., "Cassiopee: A CFD pre- and post-processing tool," *Aerospace Science and Technology*, Vol. 45, No. Supplement C, 2015, pp. 272 - 283.
[52] M. Soismier, "Stratégie de résolution hybride structurée / non structurée pour la simulation d'effets technologiques en turbomachines", Thèse de doctorat en Mécanique des fluides Energétique, France, *PhD Thesis*, 2016
[53] B. Ortun, "A coupled RANS/lifting-line analysis for modelling the aerodynamics of distributed propulsion", *AHS Aeromechanics & Design for Transformative Vertical Flight*, San Francisco, CA, January 16-18, 2018
[54] A. Dugeai, Y. Mauffrey, F. Sicot, "Aeroelastic capabilities of the *elsA* solver for rotating machines applications", *International Forum on Aeroelasticity and Structural Dynamics*, Paris, 2011.
[55] J. Peter, G. Carrier, D. Bailly, P. Klotz, M. Marcelet, F. Renac, "Local and global search methods for design in aeronautics", *Aerospace Lab*, Issue 2, 2011.
[56] J. Peter, R. Dwight, "Numerical sensitivity analysis for aerodynamic optimization: A survey of approaches", *Computers & Fluids*, Vol. 39, Issue 3, pp. 373-391, 2010.
[57] David Hue, Quentin Chanzy, and Sâm Landier, "DPW-6: Drag Analyses and Increments Using Different Geometries of the Common Research Model Airliner, *Journal of Aircraft*, Vol. 55, N° 4, July-August 2018
[58] Riéra, W., Castillon, L., Marty, J., and Leboeuf, F., "Inlet condition effects on the tip clearance flow with Zonal Detached Eddy Simulation". *Journal of Turbomachinery*, 136(4)(041018), April, pp. 1–10. Editor: R. Bunker, 2014.
[59] Riéra, W., Marty, J., Castillon, L., and Deck, S., "Zonal detached-eddy simulation applied to the tipclearance flow in an axial compressor". *AIAA Journal*, 54(8), August, pp. 2377–2391, 2016.
[60] Menter, F., and Egorov, Y., "A scale-adaptive simulation model using two-equation models". In 43rd AIAA Aerospace Sciences Meeting and Exhibit. AIAA 2005-1095. Reno, Nevada, 2005.
[61] Gourdain, N., Ottavy, X., and Vouillarmet, A., "Experimental and Numerical Investigation of Unsteady Flows in a High-Speed Three Stages Compressor," *8th European Turbomachinery Conference*, VKI, Belgium, 2009, pp. 247–266.
[62] Arnal, D., "Transition prediction in transonic flow," *Symposium Transsonicum III, Springer, 1989, pp. 253–262.*
[63] L. Pascal, G. Delattre, H. Deniau, "Implementation of stability-based transition model by means of transport equations", in *AIAA Aviation 2019 Forum*, 17-21 June 2019, Dallas, Texas.
[64] Arnal, D., Habiballah, M., and Coustols, E., "Théorie de l'instabilité laminaire et critères de transition en écoulement bi et tridimensionnel" *La Recherche Aérospatiale, Vol. 2, 1984, pp. 125–143.*
[65] Gleyzes, C., Cousteix, J., and Bonnet, J. L., "Theoretical and experimental study of low Reynolds number transitional separation bubbles," *Conference on Low Reynolds Number Airfoil Aerodynamics, Notre Dame, IN, 1985, pp. 137–152.*
[66] P.R. Spalart et al., "A new version of Detached-eddy Simulation, resistant to ambiguous grid densities," *Theoretical and Computational Fluid Dynamics*, vol. 20, pp. 181-195, 2006.
[67] F. Huvelin, S. Dequand, A. Lepage, C. Liauzun, "On the Validation and Use of High-Fidelity Numerical Simulations for Gust Response Analysis", in *Aerospace Lab*, Issue 14, 2018.
[68] Castells, F. Richez, M. Costes, "Numerical Analysis of RPM effect on Dynamic Stall Phenomena on Helicopter Rotor at High Thrust Forward Flight", *American Helicopter Society*, 2019.
[69] D. Hue, C. François, J. Dandois, A. Gebhardt, Francois "Simulations of an aircraft with constant and pulsed blowing flow control at the engine/wing junction", in *Aerospace Science and Technology Journal*, 69, 659-673, 2017.